Applied Catalysis A, General 564 (2018) 142–146

Contents lists available at ScienceDirect

Applied Catalysis A, General

journal homepage: www.elsevier.com/locate/apcata

Catalytic oxidation of NO to NO_2 for nitric acid production over a Pt/Al_2O_3 catalyst

Ata ul Rauf Salman[a], Bjørn Christian Enger[b], Xavier Auvray[a,1], Rune Lødeng[b], Mohan Menon[c], David Waller[c], Magnus Rønning[a,*]

[a] Department of Chemical Engineering, Norwegian University of Science and Technology (NTNU), Sem Sælands vei 4, NO-7491 Trondheim, Norway
[b] SINTEF Industry, Kinetic and Catalysis group, P.O. Box 4760, Torgarden, NO-7465 Trondheim, Norway
[c] YARA Technology Center, Herøya Forskningspark, Bygg 92, Hydrovegen 67, NO-3936 Porsgrunn, Norway

ARTICLE INFO

Keywords:
NO oxidation
Pt/Al_2O_3
Nitric acid
Ostwald process
Reaction order
Kinetics

ABSTRACT

The oxidation of nitric oxide (NO) to nitrogen dioxide (NO_2) is a key step both in NOx abatement technologies as well as in the Ostwald process for nitric acid production. A 1 wt.% Pt/Al_2O_3 catalyst was used to study oxidation of nitric oxide at two different concentrations of NO; 400 ppm NO (representative of engine exhaust treatment) and 10% NO (nitric acid plant). The catalyst was characterised using N_2 adsorption and CO chemisorption. The effect of temperature and feed concentration on catalytic activity was investigated.

For a feed comprising of 10% NO and 6% O_2, Pt/Al_2O_3 exhibits significant catalytic activity above 300 °C. Addition of 15% H_2O in the feed had an insignificant effect on activity of the catalyst. We report for the first time the kinetics for oxidation of NO to NO_2 under nitric acid plant conditions. An apparent activation energy of 33 kJ/mol was observed. The rate equation for the overall reaction was determined to be $r = k_f K_O (P_{O_2})^{0.5}$, where k_f is the forward rate constant. The reaction is independent of NO concentration while it has half order dependency on oxygen. The reaction mechanism which fits our experimental observation consists of dissociative adsorption of oxygen, associative adsorption of nitric oxide with desorption of nitrogen dioxide as the rate limiting step.

1. Introduction

Nitric acid is an important commodity chemical, mainly consumed for production of nitrogenous fertilizers. Commercial production takes place via the Ostwald process, consisting of three important chemical steps, (a) Oxidation of ammonia over a Pt/Rh gauze catalyst (b) Gas phase oxidation of NO into NO_2 (c) Absorption of NO_2 into water to yield nitric acid [1].

Oxidation of NO, governed by Eq. (1),

$$2NO + O_2 \leftrightharpoons 2NO_2 \quad \Delta rH_{298} = -113.8\ kJ/mol \tag{1}$$

is one of very few third order reactions and is peculiar in the sense that it has an inverse dependence on temperature [2]. According to Le Chatelier's principle, the forward reaction is favoured by low temperature and high pressure. Formation of NO_2 is favoured both kinetically and thermodynamically by low temperatures.

In the Ostwald process, typical gas composition at the exit of the ammonia combustion step is 10% NO, 6% O_2 and 15% H_2O [1]. Gas phase oxidation of nitric oxide occurs in tubing and heat exchangers downstream of the NH_3 oxidation reactor, cooling down the reaction mixture to favour the forward reaction. Use of a catalyst to oxidise nitric oxide has several advantages: a) It will accelerate the oxidation process, b) Capital costs may be reduced due to replacement of a bulky homogeneous process with a more compact heterogeneous catalytic process, c) It will enable significant heat recovery and d) Increased absorption column throughput. Despite past efforts, no catalyst that is effective under industrial conditions has been found and implemented [1]. To the best of our knowledge, except from one early patent, no published studies exists dealing with catalytic oxidation of nitric oxide at typical nitric acid plant conditions [3].

Catalytic oxidation of NO is a vital step in lean NO_x abatement technologies such as NO_x storage and reduction (NSR) [4] and selective catalytic reduction (SCR) [5]. Oxidation of nitric oxide over supported catalysts has been studied at feed concentrations varying over a wide range from 100–1500 ppm NO and 0.1–30% O_2 [6]. Various catalysts have been investigated including noble metals [7–9], metal oxides

* Corresponding author.
E-mail address: magnus.ronning@ntnu.no (M. Rønning).
[1] Current address: Competence Centre for Catalysis, Chemical Engineering, Chalmers University of Technology, S-412 96 Gothenburg, Sweden.

https://doi.org/10.1016/j.apcata.2018.07.019
Received 30 May 2018; Received in revised form 2 July 2018; Accepted 16 July 2018
Available online 17 July 2018
0926-860X/

[10–12] and perovskites [13,14]. The performance of catalysts for NO oxidation at such conditions have been reviewed by Russel and Epling [15] and Hong et al. [16].

Platinum is known to be an excellent oxidation catalyst [17]. Platinum catalysts on different support phases were shown to exhibit NO oxidation activity in the following order: $SiO_2 > Al_2O_3 > ZrO_2$ [18]. The reaction is kinetically limited at lower temperatures while at higher temperatures thermodynamics limit the conversion. NO oxidation catalysed by supported platinum catalysts is strongly dependent on Pt particle size, with higher NO oxidation rates observed for larger Pt particles. Smaller Pt particles oxidise more easily than larger ones, leading to a decrease in the number of active sites and hence lower overall catalytic activity [7,19].

It has been claimed that the catalytic activity of platinum for NO oxidation increases with O_2 concentration up to 10% while an increase in NO concentration lowers the conversion [6]. Kinetics of NO oxidation on platinum for diesel exhaust treatment has been investigated by many authors [7,20–26]. Mulla et al. [23] studied kinetics in dry feed conditions and reported a global power rate equation of the form $r = k[NO]^1[O_2]^1[NO_2]^{-1}$ demonstrating the inhibition effect of NO_2 [23]. Presence of water in the feed results in a decrease in conversion and has been attributed to competitive adsorption of water [27–29], but kinetics remain unchanged [30].

Here we report catalytic oxidation of nitric oxide using a dry feed (10% NO, 6% O_2) and wet feed (10% NO, 6% O_2 and 15% H_2O) at atmospheric pressure simulating nitric acid plant conditions. A 1 wt.% Pt/Al_2O_3 catalyst was used in this study. The design of the experimental setup capable of replicating industrial conditions in laboratory scale and investigating catalytic activity is discussed. Experimental setup was validated by reproducing the activity at typical diesel exhaust conditions (400 ppm NO) and compared with literature. The studies at nitric acid plant conditions (10% NO) show promising catalytic activity. Furthermore, the reaction orders and activation energy were investigated and a reaction mechanism is proposed.

2. Experimental

2.1. Catalyst preparation

The γ-Al_2O_3 support (Puralox SCCA. Sasol GMBH) was pre-calcined at 750 °C for 2 h in air and impregnated with 1 wt.% Pt using a one-step incipient wetness impregnation by an aqueous solution of platinum nitrate $Pt(NO_3)_4$ (Alfa Aesar, 15 wt.% solution). The material was thereafter dried in ambient air at 120 °C overnight before calcination in a flow of dry air (170 Ncm^3/min), heating at 10 °C/min from ambient to 600 °C, holding for 2 h and subsequently cooled inside the calcination reactor. The calcined material was ground and sieved to give a particle size fraction in the range 53–90 µm.

2.2. Surface area measurement

BET surface area was measured by N_2 adsorption using a Micromeritics TriStar 3000 instrument. The sample (100 mg) was degassed at 200 °C overnight prior to measurements. The specific surface areas and pore volumes were calculated using the BET [31] and BJH (desorption) methods [32,33].

2.3. Dispersion measurements

CO adsorption isotherms were recorded on a Micromeritics ASAP 2010S unit at 35 °C. A sample of 250 mg was loaded into a U-shaped reactor with an external thermocouple for temperature control. The sample was dried and evacuated at 100 °C for 30 min and reduced in flowing hydrogen by heating at 10 °C/min from ambient to 450 °C and holding for 2 h. After reduction, the sample was evacuated for 30 min at 450 °C followed by evacuation for 30 min at 35 °C. The CO adsorption isotherm was measured in the pressure range of 150–400 mmHg. After measurement of the first isotherm, the sample was degassed, followed by a second CO adsorption isotherm. The dispersion was calculated based on strongly adsorbed CO, assuming a CO/Pt adsorption ratio of 1.

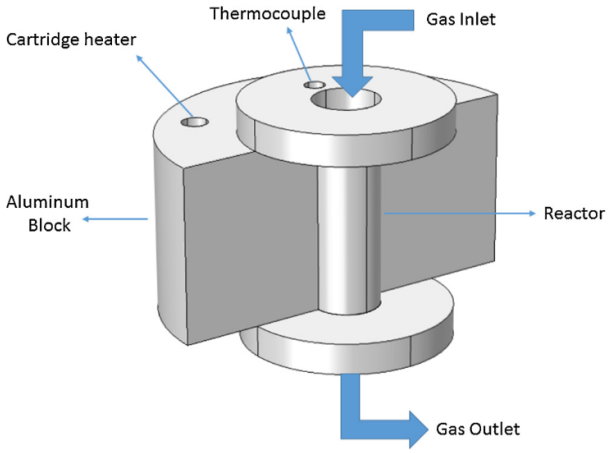

Fig. 1. Design of reactor.

The average Pt particle size was calculated using the following equation, assuming cubic particles [34].

$$d_{Pt}\ (nm) = 0.821/D_{Pt} \quad (2)$$

where D_{Pt} is platinum dispersion, determined by CO adsorption and d_{Pt} is average particle size.

2.4. Experimental set-up

There are some obvious challenges in replicating this industrial process in the laboratory. High concentrations of NO (10%) favour gas phase reactions. It is crucial to minimise such gas phase contributions in order to study the catalytic activity. The reactor design is illustrated in Fig. 1. A vertical stainless-steel tubular reactor (ID = 9.7 mm) was installed between two semi-cylindrical heat-equalizing aluminium blocks. Four cartridge heaters were inserted into the aluminium block at equal distances from the reactor axis to ensure uniform heating. The temperature in each block was measured by a K-type thermocouple close to the reactor confirming uniform heating. The temperature in the catalyst bed was controlled by a K-type thermocouple inserted into the bed from the top of the reactor, shielded from the bed by a stainless-steel sleeve.

Fig. 2 shows a simplified flow diagram for the experimental setup. Reactant gases were obtained from AGA AS (1000 ppm NO/Ar, 40% NO/Ar, 40% O_2/Ar) and argon (AGA AS, 99.99999%) was used as inert gas. Gases were controlled using Bronkhorst mass-flow controllers. All gases were individually heated to 200 °C and mixed at the inlet of the reactor. A 3-way valve was used to bypass the reactor, thus also enabling feed gas analysis. Water was introduced into the feed stream by evaporating pressurized deionized water using a Controlled Evaporator Mixer (Bronkhorst).

The product gases were diluted with 800 Ncm^3/min of argon at the reactor exit to minimize gas phase reactions and quench the temperature to 191 °C. Inlet and outlet gas concentration were analysed by an infrared gas analyser (MKS 2030-HS, 5.11 m path length, 1 bar and 191 °C).

2.5. Catalytic activity measurements

The catalyst was mixed with SiC (53–90 µm) to minimize axial temperature gradients caused by NO oxidation. The catalyst sample was placed between two quartz wool plugs inside the reactor to keep the sample in place. The total feed flow was fixed at 200 Ncm^3/min. The

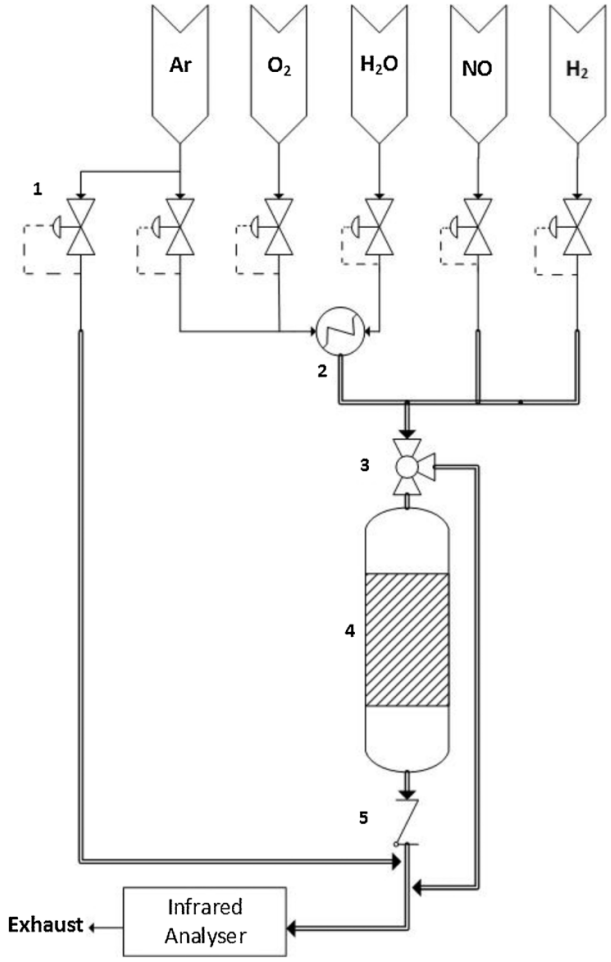

Fig. 2. Process flow diagram of experimental setup 1. Flow indicator and controller 2. Evaporator 3. Three-way valve 4. Reactor 5. One way valve, = heated line.

catalyst was activated by heating from ambient temperature at 10 °C/min in 200 Ncm^3/min of 7.5% H_2 /Ar and maintained at 450 °C for 2 h.

For investigation at diesel exhaust conditions, 100 mg of catalyst was mixed with 1.1 g SiC corresponding to a space velocity of 217,000 h^{-1}. For nitric acid plant conditions, 500 mg of catalyst was mixed with 2.75 g SiC corresponding to a space velocity of 43,400 h^{-1}.

Initial tests were performed using a feed consisting of 6% O_2, 15% H_2O (when used) mixed with NO and Ar. Two different concentration levels of NO were studied, representing diesel exhaust oxidation and industrial nitric acid production, respectively: 1) 400 ppm NO, and 2) 10% NO. Blank tests were performed without catalyst to measure and evaluate contributions from the gas phase, empty reactor and tubing. When present, this contribution was subtracted to target the catalytic conversion.

Conversion of NO to NO_2 was calculated by the following equation

$$NO\ Conversion\ [\%] = \alpha * \frac{[NO_2]_{outlet}}{[NO]_{inlet}} * 100 \quad (3)$$

Where $[NO_2]_{outlet}$ and $[NO]_{inlet}$ are concentrations of NO_2 at outlet and NO at inlet of the reactor, respectively. Constant "α" accounts for volume change with the reaction [35] where α = 0.99996 and 0.99 for diesel exhaust and nitric acid plant conditions respectively.

The effect of temperature on catalyst activity was measured by performing NO oxidation in the range 100–450 °C at atmospheric pressure. At diesel exhaust conditions, due to slow changes in the adsorption of low levels of NO, increments of 50 °C were followed by stabilization for 30 min to achieve steady state. At nitric acid plant conditions, the temperature was increased at 5 °C/min.

For calculation of apparent activation energy and reaction orders, NO conversion was restricted below 15%. Use of the Weisz-Prater criterion [36] confirmed that the system is free from internal diffusion limitations at the applied conditions. External mass and heat transfer limitations were checked by calculating the Carberry number (Ca) and using appropriate criteria suggested by Mears [37], The Ca number was found to be in the order of 10^{-5}(< < 0.05) indicating absence of any external limitations.

The apparent activation energy was calculated using an Arrhenius plot based on data obtained in the range 279–354 °C. The feed composition was maintained at 10% NO and 6% O_2 in argon, keeping the GHSV at 43,400 h^{-1}.

For reaction order measurements, approach to equilibrium (β) [26] was calculated as (P^2_{NO2}/ ($P^2_{NO}P_{O2}$ K_{eq}(T)), where K_{eq} is the equilibrium constant and the values of β were in the range (0.001-0.032) showing that the reaction is far from equilibrium at the applied conditions at 300 °C.

To obtain a rate expression, experimental conditions were selected to enable calculation of the order of reaction. The reactions were started using a feed of 10% NO and 6% O_2 in Ar at 300 °C and maintained for 2 h until stable conversion was achieved. The reactant concentration was then varied in the ranges 5–11 % NO and 3–9 % O_2 at constant space velocity. After an initial loss in activity, NO conversion was largely stabilized, therefore, each condition was maintained for 10 min to achieve steady state before collecting data. To target the conversion attributed to the catalyst, this procedure was repeated without catalyst present for comparison.

3. Results and discussion

Table 1 lists the surface area, dispersion and particle size of the catalyst. A significant drop in surface area of Al_2O_3 occurred after precalcination. The impregnation step with Pt had no impact on the total surface area of the calcined alumina.

Blank tests performed at diesel exhaust oxidation conditions (400 ppm NO) indicated no occurrence of gas phase conversion, highlighting positive impact of efforts to reduce gas phase conversion. In contrast, some authors have reported contributions from the gas phase at similar conditions [19,22,25,26]. Fig. 3 shows oxidation of 400 ppm NO with 6% O_2 over Pt/Al_2O_3 as a function of temperature. At low temperatures, the conversion increases with temperature and the reaction is kinetically limited. At 300 °C, maximum conversion is achieved and above this the reaction becomes thermodynamically limited. The slight difference between experimental values and the equilibrium curve is attributed to inaccuracies in temperature measurements. The results are comparable with earlier reports using supported platinum catalysts at diesel exhaust conditions [6,19,20,25].

Fig. 4 shows the conversion of NO as a function of temperature at nitric acid plant conditions (10% NO and 6% O_2). During the blank run, gas phase conversion decreases with increasing temperatures exhibiting an inverse Arrhenius behaviour [2]. This negative dependence of gas phase reaction on temperature confirms the inertness of the stainless-

Table 1
BET surface area from N_2 adsorption, Pt dispersion and corresponding particle size from CO chemisorption measurements.

Sample	Surface Area BET [m^2/g]	Dispersion D_{Pt} [%]	Particle Size d_{Pt} [nm]
Fresh $\gamma-Al_2O_3$	176	–	–
Calcined $\gamma-Al_2O_3$	141	–	–
Pt/Al_2O_3	141	17.7	4.6

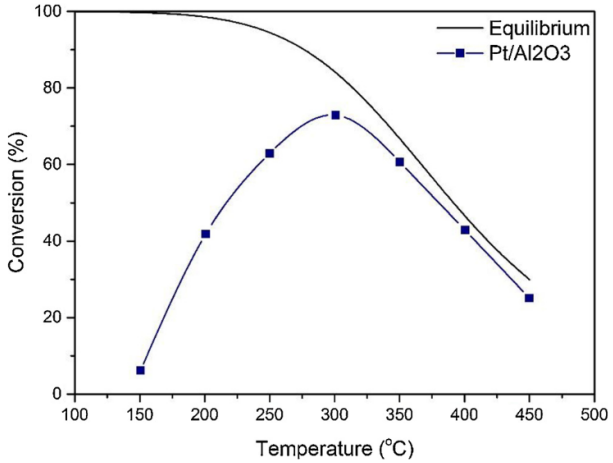

Fig. 3. Conversion of NO to NO_2 as a function of temperature for a feed: 400 ppm NO and 6% O_2 in argon.

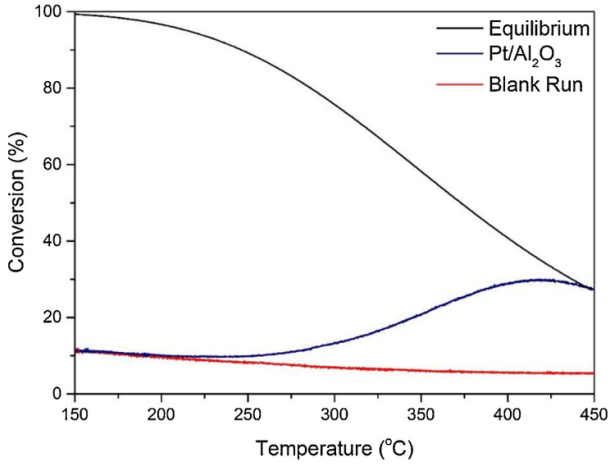

Fig. 4. Conversion of NO to NO_2 as a function of temperature for a feed: 10% NO and 6% O_2 in argon.

steel walls and surfaces. At 300 °C, about 10% NO conversion was observed. Controlled tests were carried out by filling the reactor with SiC and Al_2O_3/SiC, which confirmed their inertness. Oxidation of NO over Pt/Al_2O_3 starts to increase around 250 °C demonstrating the Arrhenius behaviour of the catalyst surface reactions. Maximum conversion is achieved around 410 °C where the reaction becomes thermodynamically limited. The fact that gas phase reactions have a negative dependence on temperature makes it easier to study catalytic activity at higher temperatures.

To study the effect of water, activity tests were conducted in wet feed (10% NO, 6% O_2 and 15% H_2O) and an insignificant effect of water was observed. A near identical conversion curve was obtained as for dry feed as shown in Fig. 4.

Comparison of turn-over frequency (TOF) at 300 °C shows a fivefold increase from 0.04 s^{-1} at diesel exhaust conditions to 0.20 s^{-1} at nitric acid plant conditions. This increase corresponds to the fivefold decrease in space velocity between the two conditions from 217,000 to 43,400 h^{-1}. Due to significant differences in feed composition and space velocity, absolute comparison is not possible but it suggests that the catalyst exhibit superior intrinsic activity at lower space velocities and higher concentrations of NO. Moreover, in comparison with diesel exhaust conditions, catalytic conversion of 10% NO starts at 250 °C. These results suggest a change in kinetics and reaction mechanism for NO oxidation at higher NO concentrations.

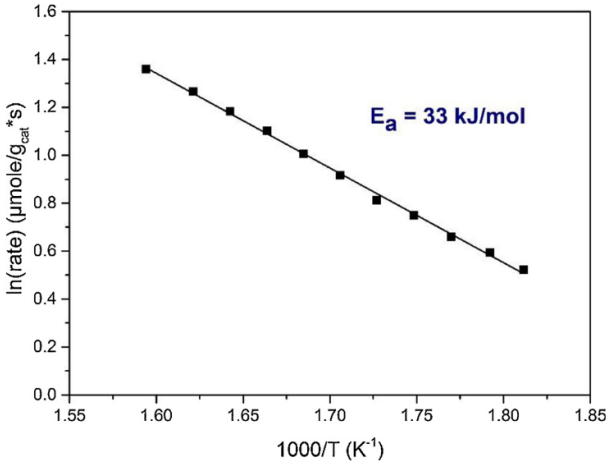

Fig. 5. Arrhenius plot for NO oxidation on Pt/Al_2O_3 for a feed of 10% NO, 6% O_2 in balance Ar.

Fig. 5 shows the effect of temperature on NO oxidation rate. An apparent activation energy (E_a) of 33 kJ/mol is obtained. Schmitz et al. [25] and Mulla et al. [23] reported values of 35 kJ/mol and 39 kJ/mol respectively for Pt/Al_2O_3 catalyst at diesel exhaust conditions, for a reaction feed free of nitrogen dioxide. Despite significant differences in feed composition and space velocities in the current study and previous works, the observed activation energies are in good agreement.

As shown in Fig. 6, the reaction shows a reaction order close to 0.5 for oxygen while it is independent of NO. Studies conducted at diesel exhaust oxidation conditions have reported reaction orders of 1, 1 and -1 for NO, O_2 and NO_2, respectively [7,23], when the feed concentrations varied from 100 to 450 ppm NO and with O_2 in the range 5–25% [23]. Molecular adsorption of O_2 was assumed as the rate determining step and chemisorbed oxygen as the Most Abundant Reaction Intermediate (MARI) for the proposed reaction mechanism explaining experimental observations [7,23]. Experimental observation of oxygen starting to desorb at 300 °C on Pt/Al_2O_3 [24] contradicts the proposed assumption of chemisorbed oxygen as MARI. Other mechanisms have been proposed as well. Olsson et al. [24] have proposed a Langmuir-Hinshelwood model with the surface reaction ($NO^* + O^* \rightarrow NO_2^* + *$) as the rate determining step [24].

In this study, with a high concentration of NO and near stoichiometric amounts of oxygen, the results suggest that the assumption that

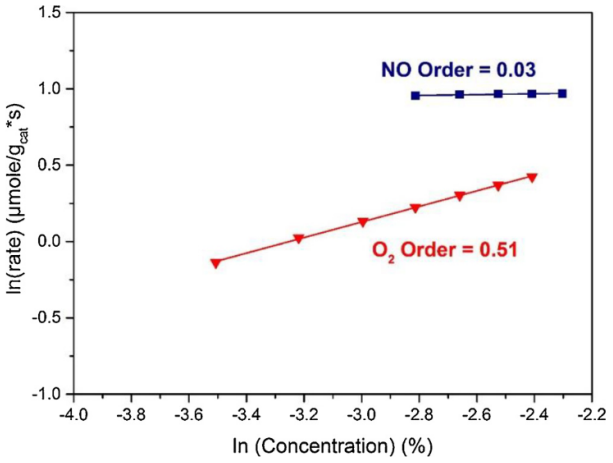

Fig. 6. Effect on NO and O_2 concentration on rate of NO oxidation at 300 °C. Feed for NO order; 5–11% NO and 6% O_2. Feed for O_2 order; 10% NO and 3–9% O_2.

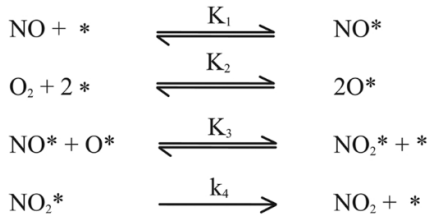

Scheme 1. Proposed NO Oxidation mechanism.

O_2 is involved in the rate-limiting step is unlikely. On Pt/Al_2O_3, dissociative adsorption of O_2 has an activation energy barrier while adsorption of NO has no activation barrier [24]. NO_2 has a high sticking coefficient and preferentially adsorbs on Pt surface sites [38,39]. Based on our findings of reaction orders and the properties of O_2, NO and NO_2, we propose the reaction mechanism in Scheme 1.

Here * represents a vacant Pt active site, k_i and K_i denote the rate constant and equilibrium constant of the ith step, respectively. By assuming step 4 as the rate determining step and NO as the MARI, the rate expression becomes

$$r = \frac{k_4 k_1 (k_2)^{0.5} k_3 P_{NO} (P_{O_2})^{0.5}}{(1 + k_1 P_{NO})} \quad (4)$$

when $K_1 P_{NO} \gg 1$, implying that the surface coverage of NO is higher than the free sites, the rate equation simplifies to

$$r = k_4 K_G (P_{O_2})^{0.5} \quad (5)$$

where $K_G = K_3 (K_2)^{0.5}$. The only kinetically relevant step in this case is the desorption of NO_2, and thermodynamics give the observed half order dependence on O_2 partial pressure. No other mechanism was found to satisfy the experimental observations.

4. Conclusions

Oxidation of nitric oxide was studied over a 1 wt. % Pt/Al_2O_3 catalyst at two different feed concentrations a) 400 ppm NO and 6% O_2 representative of diesel exhaust conditions and b) 10% NO, 6% O_2 and 15% H_2O (when present) simulating nitric acid plant conditions. The effect of temperature and feed concentration was investigated at nitric acid plant conditions and a reaction mechanism consistent with the experimental observations was proposed.

At the studied conditions, the apparent activation energy was found to be 33 kJ/mol. The reaction was found to follow half order dependency of O_2 and being independent of NO concentration.

In general, increasing NO oxidation rates in the nitric acid production using a platinum catalyst is possible, in particular above 250 °C, with significant and stable activity. With desorption of NO_2 as the rate limiting step, the reaction appears to be inhibited by the product, which is also reported for diesel exhaust treatment.

Acknowledgements

This publication forms a part of the iCSI (industrial Catalysis Science and Innovation) Centre for Research-based Innovation, which receives financial support from the Research Council of Norway under contract no. 237922.

References

[1] G. Honti, The Nitrogen Industry, Akademiai Kiado, 1976, pp. 400–413.
[2] D. Baulch, D. Drysdale, D. Horne, Homogeneous Gas Phase Reactions of the H2-N2-O2 System, CRC Press, 1973, pp. 285–300.
[3] W.C. Klingelhoefer, Nitric Oxide Oxidation, Google Patents, 1938.
[4] W.S. Epling, L.E. Campbell, A. Yezerets, N.W. Currier, J.E. Parks, Catal. Rev. 46 (2004) 163–245.
[5] Z. Liu, S. Ihl Woo, Catal. Rev. 48 (2006) 43–89.
[6] J. Després, M. Elsener, M. Koebel, O. Kröcher, B. Schnyder, A. Wokaun, Appl. Catal. B Environ. 50 (2004) 73–82.
[7] B.M. Weiss, E. Iglesia, J. Phys. Chem. C 113 (2009) 13331–13340.
[8] B.M. Weiss, E. Iglesia, J. Catal. 272 (2010) 74–81.
[9] X. Auvray, T. Pingel, E. Olsson, L. Olsson, Appl. Catal. B Environ. 129 (2013) 517–527.
[10] M.F. Irfan, J.H. Goo, S.D. Kim, Appl. Catal. B Environ. 78 (2008) 267–274.
[11] Y. Huang, D. Gao, Z. Tong, J. Zhang, H. Luo, J. Nat. Gas Sci. Eng. 18 (2009) 421–428.
[12] X. Li, S. Zhang, Y. Jia, X. Liu, Q. Zhong, J. Nat. Gas Sci. Eng. 21 (2012) 17–24.
[13] C.H. Kim, G. Qi, K. Dahlberg, W. Li, Science 327 (2010) 1624–1627.
[14] D.Y. Yoon, E. Lim, Y.J. Kim, J.H. Kim, T. Ryu, S. Lee, B.K. Cho, I.-S. Nam, J.W. Choung, S. Yoo, J. Catal. 319 (2014) 182–193.
[15] A. Russell, W.S. Epling, Catal. Rev. 53 (2011) 337–423.
[16] Z. Hong, Z. Wang, X. Li, Catal. Sci. Technol. 7 (2017) 3440–3452.
[17] K.L. Fujdala, T.J. Truex, J.B. Nicholas, J.W. Woo, Rational Design of Oxidation Catalysts for Diesel Emission Control, SAE International, 2008.
[18] E. Xue, K. Seshan, J.R.H. Ross, Appl. Catal. B Environ. 11 (1996) 65–79.
[19] S. Benard, L. Retailleau, F. Gaillard, P. Vernoux, A. Giroir-Fendler, Appl. Catal. B Environ. 55 (2005) 11–21.
[20] D. Bhatia, R.W. McCabe, M.P. Harold, V. Balakotaiah, J. Catal. 266 (2009) 106–119.
[21] R. Marques, P. Darcy, P.D. Costa, H. Mellottée, J.-M. Trichard, G. Djéga-Mariadassou, J. Mol. Catal. A Chem. 221 (2004) 127–136.
[22] S.S. Mulla, N. Chen, L. Cumaranatunge, G.E. Blau, D.Y. Zemlyanov, W.N. Delgass, W.S. Epling, F.H. Ribeiro, J. Catal. 241 (2006) 389–399.
[23] S.S. Mulla, N. Chen, W.N. Delgass, W.S. Epling, F.H. Ribeiro, Catal. Lett. 100 (2005) 267–270.
[24] L. Olsson, H. Persson, E. Fridell, M. Skoglundh, B. Andersson, J. Phys. Chem. B 105 (2001) 6895–6906.
[25] P.J. Schmitz, R.J. Kudla, A.R. Drews, A.E. Chen, C.K. Lowe-Ma, R.W. McCabe, W.F. Schneider, C.T. Goralski, Appl. Catal. B Environ. 67 (2006) 246–256.
[26] A.D. Smeltz, R.B. Getman, W.F. Schneider, F.H. Ribeiro, Catal. Today 136 (2008) 84–92.
[27] X. Auvray, L. Olsson, Appl. Catal. B Environ. 168–169 (2015) 342–352.
[28] W. Hauptmann, M. Votsmeier, J. Gieshoff, A. Drochner, H. Vogel, Appl. Catal. B Environ. 93 (2009) 22–29.
[29] L. Olsson, M. Abul-Milh, H. Karlsson, E. Jobson, P. Thormählen, A. Hinz, J. Catal. 30 (2004) 85–90.
[30] S.S. Mulla, N. Chen, L. Cumaranatunge, W.N. Delgass, W.S. Epling, F.H. Ribeiro, Catal. Today 114 (2006) 57–63.
[31] S. Brunauer, P.H. Emmett, E. Teller, JACS 60 (1938) 309–319.
[32] E.P. Barrett, L.G. Joyner, P.P. Halenda, JACS 73 (1951) 373–380.
[33] S. Lowell, J.E. Shields, M.A. Thomas, M. Thommes, Characterization of Porous Solids and Powders: Surface Area, Pore Size and Density, Kluwer Academic Publishers, 2004.
[34] M.G. White, Heterogeneous Catalysis, Prentice Hall, Englewood Cliffs, NJ, 1991 pp. 88.
[35] H. Fogler, Elements of Chemical Reaction Engineering, Prentice-Hall of India, New Delhi, 2006 pp. 92.
[36] P.B. Weisz, C.D. Prater, W.G. Frankenburg, V.I. Komarewsky, E.K. Rideal (Eds.), Advances in Catalysis, Academic Press, 1954, pp. 143–196.
[37] D.E. Mears, J. Catal. 20 (1971) 127–131.
[38] D.H. Parker, B.E. Koel, J. Vac. Sci. Technol. A 8 (1990) 2585–2590.
[39] J. Segner, W. Vielhaber, G. Ertl, Isr. J. Chem. 22 (1982) 375–379.